

Opinion piece

CrossMark
click for updates

Article submitted to journal

Subject Areas:

The 21-cm signal of hydrogen from cosmic dawn and dark ages

Keywords:

First stars, nature of dark matter, radio astronomy

Author for correspondence:

Anastasia Fialkov

e-mail: afialkov@ast.cam.ac.uk

Cosmic mysteries and the hydrogen 21-cm line: bridging the gap with lunar observations

A. Fialkov^{1,2}, T. Gessey-Jones^{2,3} and J. Dhandha^{1,2}¹Institute of Astronomy, University of Cambridge, Madingley Road, Cambridge, CB3 0HA, UK²Kavli Institute for Cosmology, Madingley Road, Cambridge, CB3 0HA, UK³Astrophysics Group, Cavendish Laboratory, J. J. Thomson Avenue, Cambridge, CB3 0HE, UK

The hydrogen 21-cm signal is predicted to be the richest probe of the young Universe including eras known as the cosmic Dark Ages, Cosmic Dawn when the first star and black hole formed, and the Epoch of Reionization. This signal holds the key to deciphering processes that take place at the early stages of cosmic history. In this opinion piece, we discuss the potential scientific merit of lunar observations of the 21-cm signal and their advantages over more affordable terrestrial efforts. The Moon is a prime location for radio cosmology which will enable precision observations of the low-frequency radio sky. The uniqueness of such observations is that they will provide an unparalleled opportunity to test cosmology and the nature of dark matter using the Dark Ages 21-cm signal. No less enticing is the opportunity to obtain a much clearer picture of Cosmic Dawn than what is achievable from the ground, which will allow us to determine the properties of the first stars and black holes.

1. The present-day landscape

We are fortunate to live in an era of spectacular successes in observational cosmology. Large-scale imaging surveys like BOSS [1], DES [2], DESI [3] and the recently launched *Euclid* [4] are able to scan the nearby Universe in great detail and map out the positions of billions of galaxies. At the same time, intensity mapping experiments such as MeerKAT [5,6], CHIME [7] and Tianlai [8] aim to provide complementary information by probing the large-scale distribution of neutral hydrogen in galaxies [5,6,9]. Combined, all these surveys provide expansive maps of our cosmic neighborhood, covering the observable Universe all the way out to redshift $z \sim 3$, when the Universe was merely 2 Gyr old. In addition to these low redshift probes, observations of the Cosmic Microwave Background (CMB), e.g. with the *Planck* satellite, provide a comprehensive picture of the Universe when it was only 0.38 million years old ($z \sim 1000$) [10].

The era between low-redshift observations and the much higher-redshift CMB last scattering surface is less well probed. Epochs such as Cosmic Dawn and the Dark Ages, forming the first few 100 million years of cosmic history, remain largely unobserved. These epochs host a large number of cosmological milestones and landmark astronomical events, such as the build-up of the first dark matter halos massive enough to hold gas, the birth of the first stars and black holes, and the onset of reionization of neutral gas by UV stellar photons which is often referred to as "the last phase transition" of the Universe [11]. The promise of exciting scientific discoveries sparks the enormous interest of the observational community in probing these epochs and motivates the launch and design of new telescopes.

However, the high-redshift Universe is notoriously difficult to observe. The high required sensitivity of galactic surveys [12–14], presence of bright Galactic [15,16] and extragalactic [17,18] foregrounds in the radio sky (see [19] for a recent review), and systematics [20–22, for example] prove to be a significant challenge. Despite this, the scientific community is actively pushing the observational frontier to earlier cosmic times. The recent launch and subsequent observations by the JWST have begun probing the bright galaxy population deep into the Epoch of Reionization at $z > 10$, pushing the limits of its predecessor, the Hubble Space Telescope (HST). Large JWST fields such as CEERS [23], GLASS and JADES have revealed hundreds of candidate galaxies at such early epochs, with the current record holder for the most distant spectroscopically confirmed object at $z \sim 13.2$ being JADES-GS-z13-0 [24,25]. Furthermore, we are beginning to see the "monsters" inhabiting the early Universe: supermassive black holes [26,27], high redshift quasars [28,29] with a record-breaking X-ray luminous quasar UHZ1 at $z = 10$ [30,31], and Active Galactic Nuclei (AGN) all the way out to the exceptionally luminous GN-z11 at $z = 10.6$ [32,33].

Despite these successes, we are merely probing the tip of the iceberg. The observations by the JWST leave out the most typical galaxies, which are dimmer than the threshold JWST sensitivity. Such galaxies are expected to be numerous and collectively may have had a strong influence on the state of the early Universe. The 21-cm signal of neutral hydrogen is expected to probe this population of galaxies by measuring their impact on the thermal and ionization histories.

2. The science-rich 21-cm signal

The 21-cm signal of neutral hydrogen from the intergalactic medium (IGM) is predicted to be the most sensitive probe of the Universe at the Epoch of Reionization and Cosmic Dawn, and the sole probe of the Dark Ages. Once detected, this signal will provide a three-dimensional map of the Universe at the broad redshift range $z \sim 6 - 1000$ [11,34,35] (note that contrary to the common assumption, although the signal at very high redshifts is weak, it is non-vanishing owing to the departure of Ly α color temperature from gas temperature [36,37]), corresponding to redshifted radio signals at $\sim 1 - 200$ MHz frequencies.

This signal, demonstrated in Figure 1, is a rich probe of astrophysics and cosmology. The top panel shows the sky-averaged (or global) 21-cm signal which can be used to determine the timing of cosmic milestones (e.g. the onset of star formation, the moment when X-ray binaries re-heated

the IGM to the temperature of the CMB, and the end of reionization). The bottom panel shows the lightcone, i.e. spatial and temporal structure of the signal. We see that the 21-cm signal is highly non-uniform at most stages of cosmic history with the fluctuation pattern changing in time as the Universe evolves and new processes dominate the signal. The figure covers several key stages in the evolution of temperature and the ionization state of the IGM including (from left to right) the Dark Ages ($z \gtrsim 30$), Cosmic Dawn ($z \sim 10 - 30$), and the entirety of the Epoch of Reionization ($z \sim 10 - 6$, with the process of reionization completed by $z \sim 5$ in this specific simulation).

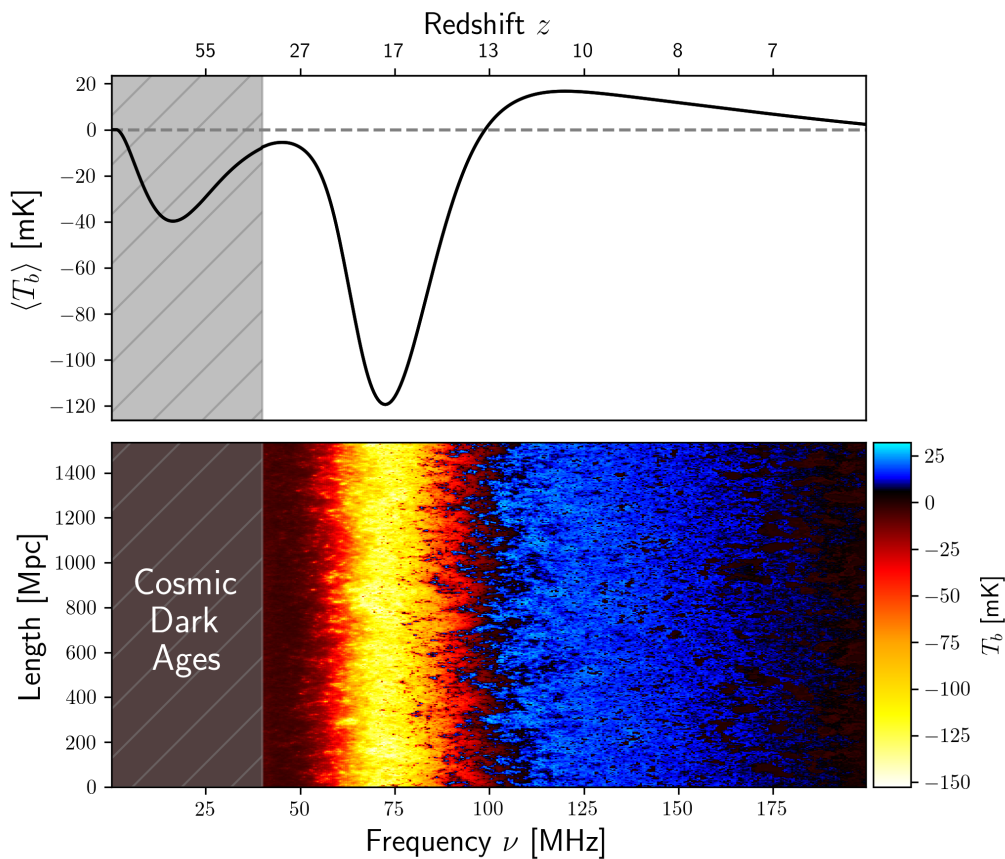


Figure 1. The 21-cm signal across cosmic time. The demonstrated timeline covers (from left to right) the Dark Ages, Cosmic Dawn, and the Epoch of Reionization, with the process of reionization completed by $z \sim 5$. We show the sky-averaged (global) signal (top) and a lightcone map of spatial fluctuations (bottom) as a function of time (horizontal) and space (vertical). The post-Dark Ages signal is generated using the semi-numerical code 21CMSPACE [38–54], while the Dark Ages global signal is generated using the analytic code RECFast++ [55, for model details]. The colorbar on the right shows the differential brightness temperature of the 21-cm line in mK. The simulations assume the standard Λ CDM cosmology with cosmological parameters from the Planck 2018 analysis [56]. In this simulation, stars are assumed to form in halos with circular velocity above 4.2 km/s. The adopted astrophysical model assumes Population III star formation with fixed 0.2% efficiency and log-flat initial mass function [52], an intermediate time-delay transition between Population III and Population II star-forming halos [51], and Population II star formation with a simple power-law efficiency [57]. X-ray binaries are assumed to produce X-rays with efficiency $f_X = 1$ and have soft SEDs with power-law exponent of -1.5 above 0.1 keV [41], while galaxies produce radio emission with an efficiency of $f_{\text{rad}} = 10$ [48]. Cosmic ionization efficiency is assumed to be of $\zeta = 15$ [58]. The simulations also include various feedback processes such as Lyman-Werner feedback [39], photo-heating [44], and baryon-dark matter relative motion [38].

The Dark Ages 21-cm signal is largely determined by structure formation and dark matter physics. This signal probes fluctuations in the baryon density, peculiar velocity, and baryon temperature. Precision modeling of the 21-cm signal from the Dark Ages requires the inclusion of cosmological phenomena such as redshift evolution (light-cone), the Alcock-Paczynski effect, the relative velocity between dark matter and gas, collisions of hydrogen atoms with various species, the color temperature of the residual Ly α photons left over from Recombination, and the distribution of the mildly (at the level of $\sim 10^{-4}$) ionized gas [36,37,59–61].

Collisional coupling between the hydrogen atoms and all existing particles throughout the cosmic dark ages guarantees that the 21-cm signal is driven by the kinetic temperature of the gas, resulting in a non-vanishing but faint radio signal visible in absorption against the CMB background [34]. Within the conventionally considered "standard" models of cosmology and astrophysics, the observable absorption feature has differential brightness $T_b \sim -40$ mK at $z \sim 75$ [61, and Figure 1 of this work]. This signal is typically much weaker than the Cosmic Dawn absorption trough which we discuss in the following paragraph (centered at $z \sim 18$ for the model demonstrated in Figure 1), but is roughly of the same brightness as the reionization emission peak which occurs in models with strong enough heating (at $z \sim 11$ for the model shown in Figure 1). Note that in scenarios with inefficient heating [41], the neutral IGM might be colder than the CMB for the entirety of cosmic history (including the Epoch of Reionization) thus resulting in the 21-cm signal seen in absorption at any redshift (i.e. with no emission feature) and "cold reionization". As the Universe expands and collisions become less efficient, the 21-cm signal fades away becoming practically undetectable (around $z \sim 30$ in Figure 1).

The next milestone in the history of the Universe is the formation of the first sources of light which ushers the Universe into the Cosmic Dawn era ($z \sim 10 - 30$). As the first stars emerge at $z \sim 30$ [62], they produce Ly α photons that couple the 21-cm spin temperature to the kinetic temperature of the gas [39,40,52,63,64]. Owing to the different adiabatic cooling rates, the gas temperature is colder than the CMB, resulting in an observable absorption signal. As the Universe expands and adiabatically cools down further, the absorption deepens – a process that continues until the first population of heating sources emerges. The onset of cosmic heating defines the so-called "absorption trough", the global minimum of the sky-averaged 21-cm signal, clearly seen in the top panel of Figure 1 at $z \sim 18$. One of the most widely considered types of heating sources are the first X-ray binaries [65,66]. These astrophysical objects are natural end-points of stellar evolution [67,68]; as the first stars die, some end up as compact objects in binary systems (e.g. the first astrophysical black holes). These systems produce X-rays in the process of accretion [66] or decretion [69] of gas. The X-ray background contributes to reheating of the IGM in a non-uniform manner (see Figure 1, [41,45,70]) and the contrast between the gas temperature and the CMB decreases. The gas can also be heated by other astrophysical sources, e.g. via cosmic rays [54,71] or Ly α scattering [49,72,73]. As we mentioned above, depending on the efficiency of the first heating sources, the neutral gas temperature might either rise above that of the background radiation resulting in an emission 21-cm signal (as shown in Figure 1 at the low-redshift end) or remain colder than that of the CMB resulting in an absorption 21-cm signal until the end of reionization [41]. Finally, the signal vanishes as the neutral hydrogen in the IGM is ionized by galaxies and quasars.

The Cosmic Dawn global 21-cm trough ($z \sim 18$ in Figure 1) might be a few hundred mK deep [47,49,74, with the exact location and depth being model-dependent] and the spatial structure of the signal is predicted to have a rich fluctuation pattern that could inform us on some of the earliest astrophysical processes [41,54,70,75]. This deep absorption is the target of many ground-based missions such as the radiometers EDGES [76], MIST [77], REACH [78], and SARAS [79], and the interferometers which target fluctuations in the 21-cm signal such as HERA [80], LOFAR [81, 82], NenuFAR [83,84], MWA [85], LWA [86], LEDA [87] as well as the future SKA [88,89].

In addition to the *commonly considered* astrophysical and cosmological processes described above, the signal will depend on other processes if they affect the growth of structure, star and black hole formation, or heating and ionization of the Universe. For instance, dark matter

cooling [46,90–93] or excess radio background above the CMB level [47,48,53,94–96] will affect the structure, magnitude and features of the signal.

3. Science with ground-based 21-cm observations

The science-rich 21-cm signal outlined above is hard to measure owing to its intrinsic faintness, the brightness of overlaying foreground signals, and the uncertainty in instrumental systematics.

Terrestrial observations of the Dark Ages are made particularly difficult by the ionosphere which corrupts low radio frequencies. Due to the electromagnetic properties of the ionosphere, signals at frequencies below $\mathcal{O}(10)$ MHz (plasma frequency of the F-layer peak) are reflected into space and cannot be observed from the ground, while radio waves below ~ 300 MHz are refracted and partially absorbed [97–99]. As a result, the cosmic Dark Ages, which are encoded in the lowest radio frequencies owing to the expansion of the Universe, can only be measured from above the ionosphere providing the most compelling science case for lunar and space missions.

Although the remaining parts of cosmic history, including the signals from Cosmic Dawn and the Epoch of Reionization, are accessible from the ground, the ionosphere acts as a lens creating chromatic distortions of the incoming low-frequency radio waves [99,100, and right panel of Figure 2]. Shen et al. [101] showed that more than 5% error in a time-dependent ionospheric model will corrupt the global 21-cm measurement (left panel of Figure 2). The ionosphere, naturally, also creates a problem for interferometric observations of fluctuations in the 21-cm signal. Ionospheric propagation delays are a major contributor to phase errors at low radio frequencies and can pose a significant challenge even for the Epoch of Reionization experiments [102]. Although currently, the impact of the ionosphere is often left untreated, the ionospheric effects can be (at least partially) removed, e.g. LOFAR is using direction-dependent calibration [103].

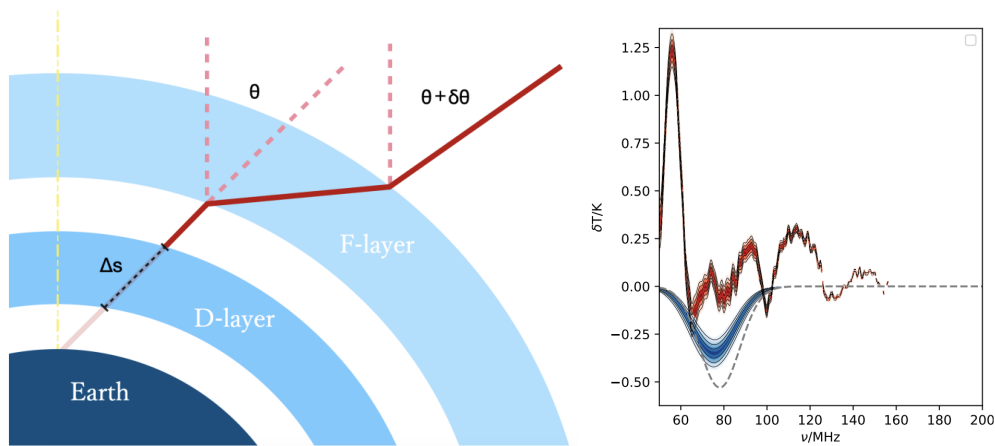


Figure 2. **Left:** Refraction and absorption of homogeneous ionospheric layers, not-to-scale, adapted from [100]. The illustration shows two layers (F-layer and D-layer) of the ionosphere that have the most important impact on radio wave propagation: the F-layer is the highest region of the ionosphere and has the highest density of free electrons thus providing the dominant contribution to refraction. Although its average degree of ionization does not vary significantly through the night, the ion distribution might vary. The D-layer dominates absorption. **Right:** Measuring the global 21-cm signal in the presence of time-varying ionosphere. The signal is extracted using a Bayesian pipeline of the REACH experiment [104]. The data includes an injected/true cosmic signal (grey dashed), residuals with the fitted foreground removed are shown in red, and the best-fit reconstructed global 21-cm signal posterior is shown in blue. Plot adapted from Shen et al. 2022 [101]. Time-varying ionosphere is implemented using the real data collected from Lowell GIRO Data Center at station Louisvale, South Africa. Shen et al. 2022 conclude that more than 5% error in the ionospheric (time-dependent) model will impede the global 21-cm measurement.

In addition to the ionospheric distortions, human-made radio frequency interference (RFI) contaminates the signal making the ground-based observations harder to interpret. These issues lead us to think that lunar observations of Cosmic Dawn and the Epoch of Reionization (especially from the lunar dark side to avoid RFI) would provide a much clearer view of the epochs and allow us to robustly extract some of the most interesting details of primordial star and black hole formation as well as shedding light on the nature of dark matter and structure formation at early times.

Despite the difficulties, many of the existing ground-based low-frequency radio telescopes provide competitive upper limits that are, in some cases, strong enough to rule out most extreme theoretical models.

A fully Bayesian analysis conducted by Bevins et al. 2023 [105] showed that, at the time of writing, HERA provides the tightest constraints on the 21-cm power spectrum from the Epoch of Reionization [106], followed closely by LOFAR [107] and MWA [108]. The latest publicly available HERA limits (at 95% confidence) are $\Delta^2 = 457 \text{ mK}^2$ at $k = 0.34 \text{ h Mpc}^{-1}$ and $z = 7.9$, and $\Delta^2 = 3496 \text{ mK}^2$ at $k = 0.36 \text{ h Mpc}^{-1}$ and $z = 10.4$, derived using 94 nights of observing with HERA Phase I. In addition to the constraints obtained using the interferometric data, residuals of the global signal experiments SARAS 2 and EDGES High-Band appear to be low enough to rule out some of the standard astrophysical scenarios at the reionization redshifts [109–112].

Observations of Cosmic Dawn are more controversial. The EDGES collaboration reported a tentative detection of a deep absorption trough at $z \sim 17$ with the EDGES Low-Band antenna [76]. This detection has not been confirmed and is in tension with SARAS 3 measurements at $z \sim 15 - 25$ [79]. Exploration of Cosmic Dawn is also being conducted with interferometers including the 'AARTFAAC Cosmic Explorer' (ACE) program of LOFAR [113], NenuFAR [84], MWA [114], LWA [86] and LEDA [87]. However, the published Cosmic Dawn power spectra limits are very weak and do not constrain any astrophysical scenarios.

The constraining data (e.g. from HERA at $z = 8$ and 10 [106] and SARAS 3 at $z \sim 15 - 25$ [79]) are being used to restrict standard and exotic astrophysical scenarios, including models with enhanced 21-cm signals boosted by the extra radio background present in addition to the CMB [47,48,53]. Such models, originally designed to explain the anomalous EDGES Low-Band detection, provide an interesting theoretical test case. In a Bayesian analysis, limits on the 21-cm power spectrum at $z \sim 8$ and 10 from HERA and global signal constraints at $z \sim 15 - 25$ from SARAS 3 were shown to limit the astrophysical parameter space of these models [105]. Bevins et al. (2023) [105] showed that in synergy, the two experiments leave only $64.9^{+0.3}_{-0.1}\%$ of the explored prior space to be consistent with the joint data set. The strongest joint constraints are in the space of the radio and X-ray luminosities of the first galaxies. The joint analysis disfavors at 68% confidence a combination of galaxies with X-ray emission that is $\lesssim 33$ and radio emission that is $\gtrsim 32$ times as efficient as present-day galaxies. In addition, weak trends in constraints of star formation efficiency and minimum halo mass for star formation are seen.

The synergetic constraints by HERA and SARAS 3 can be further supplemented by the unresolved X-ray background measurements from the *Chandra* X-ray satellite [115,116] and the radio background detected by ARCADE2 [117] and LWA1 [118]. In their work Pochinda et al. [119] considered a model that differentiates between the primordial stars (Population III, see more discussion in Section 4 (a) below) formed out of chemically pristine gas (at the Big Bang nucleosynthesis level) and second-generation stars (Population II) formed out of chemically-enriched gas. This study indicates that SARAS 3 data is (weakly) sensitive to the properties of Population III star-forming regions, while the other experiments mostly constrain the properties of X-ray and radio sources. Although very weak and model-dependent, these limits are one of the first to test the properties of primordial star-forming regions. This analysis illustrates that even the existing data, despite being plagued by systematic effects, ionospheric distortions and foreground uncertainties, can be used to advance our understanding of astrophysics at Cosmic Dawn.

4. Science from the Moon

Observations from the lunar surface or space will provide the only way to probe the state of neutral hydrogen during the Dark Ages as this radio signal is inaccessible from the ground. Moreover, these observations are expected to supersede terrestrial observations of Cosmic Dawn bypassing the issues of ionospheric distortions and radio frequency interference (if performed from the lunar dark side). Owing to the cleaner radio environment, measurements of the Cosmic Dawn 21-cm signal from the Moon might allow us to test some of the most intriguing properties of first stars and black holes.

(a) Crisp observations of Cosmic Dawn

Precise 21-cm signal measurements of Cosmic Dawn are probably our best chance to probe the first generation of stars (also called Population III or Pop III stars) and the successive population of first X-ray binaries (XRBs). Little is known for certain about these objects [62,66], but it is widely believed that the first metal-free stars form in small numbers in dark-matter mini-halos from the hydrogen and helium gas produced in Big Bang nucleosynthesis. Despite making up only a tiny fraction of the stars that will ever form, these stars should have had a profound impact on the history of the Universe, producing the first metals, and starting the reionization of the IGM. Properties of the first population of XRBs, which are responsible for the onset of the IGM heating, are tightly linked to the properties of the stars themselves (such as the stellar initial mass function (IMF) [66]).

The sensitivity of the Cosmic Dawn 21-cm signal to the first stars and XRBs, via the Ly α photon emission of the former and X-rays generated by the latter, allows it to probe these first sources of light. At the most basic level, detecting global features associated with Cosmic Dawn in the 21-cm signal, like the rapid drop in the 21-cm global signal and the subsequent rise as a result of heating (demonstrated in Figure 1), will reveal the timing and efficiency of the formation of the first stars and XRBs. Further high signal-to-noise measurements of the 21-cm signal from Cosmic Dawn should provide additional details and insights into the properties of the first sources.

For example, emissivity of a Pop III star in the Lyman band depends on the mass of the star [52,120]. As a result, the combined signature of the first stellar population in the 21-cm signal depends on the distribution of stellar masses, the so-called initial mass function (IMF, see Figure 3). Different IMFs result in small, but potentially measurable, variations in the predicted Cosmic Dawn 21-cm signal [52]. If first star formation was efficient, these signatures may be just measurable by the SKA [89], though at low signal-to-noise ratios. However, if first star formation is inefficient or occurs earlier than anticipated (e.g. in the case of rare overdense regions) these differences will require precise low-frequency 21-cm signal measurements that are only feasible from the lunar dark side.

(b) The unseen Dark Ages

The ability to probe the Dark Ages provides a unique science case for space and lunar observations of the 21-cm signal. Uncontaminated by astrophysics, it provides a new probe of fundamental physics over the unprecedentedly large range of scales and unseen cosmic time. By performing a mode counting exercise, Cole and Silk (2021) [121] found that lunar observations of the three-dimensional (nearly linear) 21-cm power spectrum from $z = 50$ will probe $\sim 10^{12}$ modes, which is considerably larger than the amount of information contained in the CMB ($\sim 10^6$ modes) and large scale structure (10^8 modes at $z = 1$).

The Dark Ages are marked by the first-ever infall of gas into newly assembled deep dark matter potential wells and, thus, provide an unprecedented opportunity to study the birth-places of first stars and the onset of structure formation [75,122]. Low-frequency radio experiments with arcminute angular resolution will be able to probe non-Gaussianity produced by nonlinear collapse e.g. using the 21-cm bispectrum [123]. Beyond these exciting prospects is the highly

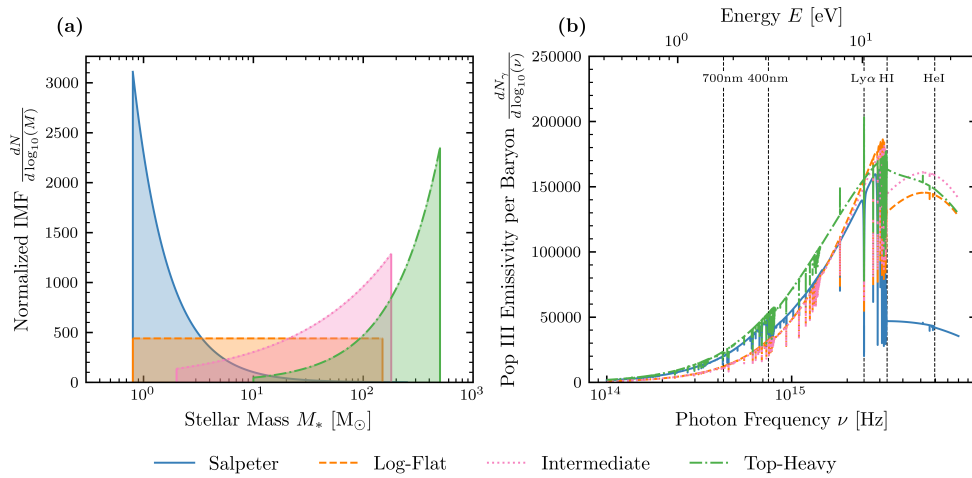


Figure 3. The emissivity of the first stars varies with their mass distribution. Panel (a, left) depicts four truncated power-law initial mass functions (IMFs) that may describe the mass distribution of the first stars. Panel (b, right) shows the corresponding prediction for the population-averaged emissivity per baryon of the first stars given these IMFs. The Lyman- α line (Ly α), hydrogen ionizing energy (HI), and helium ionizing energy (HeI) are highlighted as the emissivity above these lines has particular importance in determining the evolution of the 21-cm signal. Moderate differences are seen in emission between Ly α and HI between IMFs and significant variations in ionizing emissivity. The Lyman band emissivity variations produce potentially observable differences in the 21-cm signal [52], suggesting the possibility of probing the mass distribution of the first stars using the 21-cm signal.

compelling case of early cosmology [61]. The large number of linear modes probed by the Dark Ages 21-cm signal will provide an unparalleled test of primordial non-Gaussianity of the initial density field [123–126]. The signal from $z \sim 30 - 100$ will test the inflationary paradigm on small scales (down to ~ 0.1 Mpc) inaccessible to the CMB experiments, allowing us to probe theories with primordial non-Gaussianity of $f_{\text{NL}} \gtrsim 10^{-2}$ [123,125,127]. This constraint improves ($f_{\text{NL}}^{\text{loc}} \sim 6 \times 10^{-3}$) when cross-correlations between 21-cm fluctuations and the CMB T- and E-mode anisotropies are considered [126].

If deviations of the Dark Ages 21-cm signal from the predictions of the standard Λ CDM cosmology are observed, this could be a signature of dark matter physics [128–133], or other exotic processes [134–138]. In any theory in which new phenomena contribute to structure formation, heating or ionization at early times, these signatures will be directly imprinted in the 21-cm signal. Some examples include ultra-light axions which would affect the 21-cm signal by changing the matter power spectrum and thus affecting the collapse of early structures [133], dark matter annihilation or decay which could change temperature and ionization state of the gas [129,132], primordial black holes which impact the signal through Hawking radiation (evaporation) or emitting radiation in the process of accretion [134,136,138], and superconducting cosmic strings (e.g. [135]).

(c) Caveats

Undoubtedly, the scientific merits of the low-frequency radio observations from the lunar farside are great, with exciting prospects to probe fundamental physics, cosmology, and high-redshift astrophysics. The advantages of dark-side lunar observations are clear: the lack of ionosphere and RFI, as well as environmental stability during the two-week lunar night which permits long uninterrupted integration times [139]. However, such observations are technically challenging (see the White Paper by Koopmans et al. (2021) [140] for more details).

Low-frequency radio astronomy is plagued by the presence of bright foregrounds [16] which are several orders of magnitude stronger than the intrinsically weak 21-cm signal. This problem is a challenge for 21-cm observations from the ground and the Moon alike. The foregrounds are stronger at lower frequencies and, therefore, will be a more serious obstacle for the robust identification of the Dark Ages 21-cm signal compared to the Cosmic Dawn or Reionization eras. A viable solution is to marginalize over the foreground parameters when inferring cosmological properties [104].

Operating from the Moon also involves unfamiliar technical challenges [139,140]. For example, reflections from the lunar subsurface are not well understood [141] and could corrupt the observation if not modeled adequately. Physical properties of the lunar regolith such as density and porosity [142] could impact mission operation. Other environmental challenges include the large temperature gradients ($\sim 100^\circ\text{C}$ during the day and -170°C at night) which can destabilize instrumentation, the charged lunar dust environment [143], and micrometeoroid flux which can affect the longevity of experiments. For interferometry, to achieve the required high spatial resolution and sensitivity it is estimated that an array of 10^5 individual antennas distributed over 100 km^2 is needed [61,140,144] with integration times of up to 10,000 hours required for precision cosmology [61]. To host such large experiments, very few suitable shadowed craters exist on the lunar farside [145] adding to the need for urgent international policy in protecting these environments for astronomical research.

5. Conclusion

In this opinion piece, we reviewed the physics and the observational status of 21-cm cosmology. We provided a short discussion of the scientific merit of lunar observations at low radio frequencies arguing that the Moon, indeed, is expected to provide a unique environment for 21-cm cosmology. A plethora of exciting scientific questions can only be answered by doing 21-cm science from space/lunar surface. In particular, observations of the 21-cm signal from the cosmic Dark Ages are only possible from either space or the Moon. These unique measurements will open up a new window to study cosmology and structure formation in the unexplored regime when the first bound dark matter objects (e.g. halos) were forming. If measured, deviations from the predictions assuming the standard ΛCDM cosmology could point to the presence of "exotic" processes such as non-cold dark matter. Additionally, free from ionospheric distortions and human-made interference, observations from the Moon/space are also expected to provide a clearer view of the epoch of the first star and XRB formation than what is possible from the ground, enabling precision science at Cosmic Dawn. Specifically, robustly determining the typical masses (and hopefully the full mass distribution) of the first generation of stars is one of the most exciting scientific questions that can be answered with 21-cm cosmology from the Moon/space.

Acknowledgements. We thank the two anonymous referees for their constructive comments which helped improve the paper. AF is grateful to the Royal Society for its continuous and generous support in the form of a URF. TGJ acknowledges the support of the Science and Technology Facilities Council (STFC) through grant number ST/V506606/1. JD acknowledges support from the Boustany Foundation and Cambridge Commonwealth Trust in the form of an Isaac Newton Studentship. AF thanks C. J. O'Connell for the careful proofreading of this manuscript.

References

1. Dawson KS, Schlegel DJ, Ahn CP et al.. 2013 The Baryon Oscillation Spectroscopic Survey of SDSS-III. *AJ* **145**, 10. ([10.1088/0004-6256/145/1/10](https://doi.org/10.1088/0004-6256/145/1/10))
2. Sevilla-Noarbe I, Bechtol K, Carrasco Kind M et al.. 2021 Dark Energy Survey Year 3 Results: Photometric Data Set for Cosmology. *ApJS* **254**, 24. ([10.3847/1538-4365/abeb66](https://doi.org/10.3847/1538-4365/abeb66))
3. DESI Collaboration, Adame AG, Aguilar J et al.. 2023 The Early Data Release of the Dark Energy Spectroscopic Instrument. *arXiv e-prints* p. arXiv:2306.06308. ([10.48550/arXiv.2306.06308](https://doi.org/10.48550/arXiv.2306.06308))

4. Laureijs R, Amiaux J, Arduini S et al.. 2011 Euclid Definition Study Report. *arXiv e-prints* p. arXiv:1110.3193. ([10.48550/arXiv.1110.3193](https://doi.org/10.48550/arXiv.1110.3193))
5. Cunnington S, Li Y, Santos MG et al.. 2023 H I intensity mapping with MeerKAT: power spectrum detection in cross-correlation with WiggleZ galaxies. *MNRAS* **518**, 6262–6272. ([10.1093/mnras/stac3060](https://doi.org/10.1093/mnras/stac3060))
6. Paul S, Santos MG, Chen Z et al.. 2023 A first detection of neutral hydrogen intensity mapping on Mpc scales at $z \approx 0.32$ and $z \approx 0.44$. *arXiv e-prints* p. arXiv:2301.11943. ([10.48550/arXiv.2301.11943](https://doi.org/10.48550/arXiv.2301.11943))
7. CHIME Collaboration, Amiri M, Bandura K et al.. 2022 An Overview of CHIME, the Canadian Hydrogen Intensity Mapping Experiment. *ApJS* **261**, 29. ([10.3847/1538-4365/ac6fd9](https://doi.org/10.3847/1538-4365/ac6fd9))
8. Chen X. 2012 The Tianlai Project: a 21CM Cosmology Experiment. In *International Journal of Modern Physics Conference Series* vol. 12 *International Journal of Modern Physics Conference Series* pp. 256–263. ([10.1142/S2010194512006459](https://doi.org/10.1142/S2010194512006459))
9. Amiri M, Bandura K, Chen T et al.. 2023 Detection of Cosmological 21 cm Emission with the Canadian Hydrogen Intensity Mapping Experiment. *ApJ* **947**, 16. ([10.3847/1538-4357/acb13f](https://doi.org/10.3847/1538-4357/acb13f))
10. Planck Collaboration, Aghanim N, Akrami Y et al.. 2020 Planck 2018 results. VI. Cosmological parameters. *A&A* **641**, A6. ([10.1051/0004-6361/201833910](https://doi.org/10.1051/0004-6361/201833910))
11. Barkana R. 2016 The rise of the first stars: Supersonic streaming, radiative feedback, and 21-cm cosmology. *Phys. Rep.* **645**, 1–59. ([10.1016/j.physrep.2016.06.006](https://doi.org/10.1016/j.physrep.2016.06.006))
12. Madau P, Dickinson M. 2014 Cosmic Star-Formation History. *ARA&A* **52**, 415–486. ([10.1146/annurev-astro-081811-125615](https://doi.org/10.1146/annurev-astro-081811-125615))
13. Zackrisson E, Rydberg CE, Schaerer D et al.. 2011 The Spectral Evolution of the First Galaxies. I. James Webb Space Telescope Detection Limits and Color Criteria for Population III Galaxies. *ApJ* **740**, 13. ([10.1088/0004-637X/740/1/13](https://doi.org/10.1088/0004-637X/740/1/13))
14. Steinhardt CL, Jespersen CK, Linzer NB. 2021 Finding High-redshift Galaxies with JWST. *ApJ* **923**, 8. ([10.3847/1538-4357/ac2a2f](https://doi.org/10.3847/1538-4357/ac2a2f))
15. Davies RD, Wilkinson A. 1998 Synchrotron Emission from the Galaxy. *arXiv e-prints* pp. astro-ph/9804208. ([10.48550/arXiv.astro-ph/9804208](https://doi.org/10.48550/arXiv.astro-ph/9804208))
16. de Oliveira-Costa A, Tegmark M, Gaensler BM et al.. 2008 A model of diffuse Galactic radio emission from 10 MHz to 100 GHz. *MNRAS* **388**, 247–260. ([10.1111/j.1365-2966.2008.13376.x](https://doi.org/10.1111/j.1365-2966.2008.13376.x))
17. Best PN, Kondapally R, Williams WL et al.. 2023 The LOFAR Two-metre Sky Survey: Deep Fields data release 1. V. Survey description, source classifications, and host galaxy properties. *MNRAS* **523**, 1729–1755. ([10.1093/mnras/stad1308](https://doi.org/10.1093/mnras/stad1308))
18. Hurley-Walker N, Callingham JR, Hancock PJ et al.. 2017 GaLactic and Extragalactic All-sky Murchison Widefield Array (GLEAM) survey - I. A low-frequency extragalactic catalogue. *MNRAS* **464**, 1146–1167. ([10.1093/mnras/stw2337](https://doi.org/10.1093/mnras/stw2337))
19. Chapman E, Jelić V. 2019 Foregrounds and their mitigation. *arXiv e-prints* p. arXiv:1909.12369. ([10.48550/arXiv.1909.12369](https://doi.org/10.48550/arXiv.1909.12369))
20. Steinhardt CL, Kokorev V, Rusakov V et al.. 2023 Templates for Fitting Photometry of Ultra-high-redshift Galaxies. *ApJ* **951**, L40. ([10.3847/2041-8213/acdef6](https://doi.org/10.3847/2041-8213/acdef6))
21. Arrabal Haro P, Dickinson M, Finkelstein SL et al.. 2023 Confirmation and refutation of very luminous galaxies in the early Universe. *Nature* **622**, 707–711. ([10.1038/s41586-023-06521-7](https://doi.org/10.1038/s41586-023-06521-7))
22. Hills R, Kulkarni G, Meerburg PD et al.. 2018 Concerns about modelling of the EDGES data. *Nature* **564**, E32–E34. ([10.1038/s41586-018-0796-5](https://doi.org/10.1038/s41586-018-0796-5))
23. Finkelstein SL, Bagley MB, Ferguson HC et al.. 2023 CEERS Key Paper. I. An Early Look into the First 500 Myr of Galaxy Formation with JWST. *ApJ* **946**, L13. ([10.3847/2041-8213/acade4](https://doi.org/10.3847/2041-8213/acade4))
24. Curtis-Lake E, Carniani S, Cameron A et al.. 2023 Spectroscopic confirmation of four metal-poor galaxies at $z = 10.3$ – 13.2 . *Nature Astronomy* **7**, 622–632. ([10.1038/s41550-023-01918-w](https://doi.org/10.1038/s41550-023-01918-w))
25. Robertson BE, Tacchella S, Johnson BD et al.. 2023 Identification and properties of intense star-forming galaxies at redshifts $z > 10$. *Nature Astronomy* **7**, 611–621. ([10.1038/s41550-023-01921-1](https://doi.org/10.1038/s41550-023-01921-1))
26. Larson RL, Finkelstein SL, Kocevski DD et al.. 2023 A CEERS Discovery of an Accreting Supermassive Black Hole 570 Myr after the Big Bang: Identifying a Progenitor of Massive $z > 6$ Quasars. *ApJ* **953**, L29. ([10.3847/2041-8213/ace619](https://doi.org/10.3847/2041-8213/ace619))
27. Furtak LJ, Labbé I, Zitrin A et al.. 2023 A supermassive black hole in the early universe growing in the shadows. *arXiv e-prints* p. arXiv:2308.05735. ([10.48550/arXiv.2308.05735](https://doi.org/10.48550/arXiv.2308.05735))
28. Yue M, Eilers AC, Simcoe RA et al.. 2023 EIGER V. Characterizing the Host Galaxies of Luminous Quasars at $z \sim 6$. *arXiv e-prints* p. arXiv:2309.04614. ([10.48550/arXiv.2309.04614](https://doi.org/10.48550/arXiv.2309.04614))

29. Christensen L, Jakobsen P, Willott C et al.. 2023 Metal enrichment and evolution in four $z > 6.5$ quasar sightlines observed with JWST/NIRSpec. *A&A* **680**, A82. ([10.1051/0004-6361/202347943](https://doi.org/10.1051/0004-6361/202347943))
30. Bogdán Á, Goulding AD, Natarajan P et al.. 2023 Evidence for heavy-seed origin of early supermassive black holes from a $z \approx 10$ X-ray quasar. *Nature Astronomy*. ([10.1038/s41550-023-02111-9](https://doi.org/10.1038/s41550-023-02111-9))
31. Goulding AD, Greene JE, Setton DJ et al.. 2023 UNCOVER: The Growth of the First Massive Black Holes from JWST/NIRSpec-Spectroscopic Redshift Confirmation of an X-Ray Luminous AGN at $z = 10.1$. *ApJ* **955**, L24. ([10.3847/2041-8213/acf7c5](https://doi.org/10.3847/2041-8213/acf7c5))
32. Tacchella S, Eisenstein DJ, Hainline K et al.. 2023 JADES Imaging of GN-z11: Revealing the Morphology and Environment of a Luminous Galaxy 430 Myr after the Big Bang. *ApJ* **952**, 74. ([10.3847/1538-4357/acdbc6](https://doi.org/10.3847/1538-4357/acdbc6))
33. Bunker AJ, Saxena A, Cameron AJ et al.. 2023 JADES NIRSpec Spectroscopy of GN-z11: Lyman- α emission and possible enhanced nitrogen abundance in a $z = 10.60$ luminous galaxy. *A&A* **677**, A88. ([10.1051/0004-6361/202346159](https://doi.org/10.1051/0004-6361/202346159))
34. Furlanetto SR, Oh SP, Briggs FH. 2006 Cosmology at low frequencies: The 21 cm transition and the high-redshift Universe. *Phys. Rep.* **433**, 181–301. ([10.1016/j.physrep.2006.08.002](https://doi.org/10.1016/j.physrep.2006.08.002))
35. Mesinger A. 2019 *The Cosmic 21-cm Revolution; Charting the first billion years of our universe*. ([10.1088/2514-3433/ab4a73](https://doi.org/10.1088/2514-3433/ab4a73))
36. Fialkov A, Loeb A. 2013 The 21-cm Signal from the cosmological epoch of recombination. *J. Cosmology Astropart. Phys.* **2013**, 066. ([10.1088/1475-7516/2013/11/066](https://doi.org/10.1088/1475-7516/2013/11/066))
37. Breyse PC, Ali-Haïmoud Y, Hirata CM. 2018 Ultimate frontier of 21-cm cosmology. *Phys. Rev. D* **98**, 043520. ([10.1103/PhysRevD.98.043520](https://doi.org/10.1103/PhysRevD.98.043520))
38. Visbal E, Barkana R, Fialkov A et al.. 2012 The signature of the first stars in atomic hydrogen at redshift 20. *Nature* **487**, 70–73. ([10.1038/nature11177](https://doi.org/10.1038/nature11177))
39. Fialkov A, Barkana R, Visbal E et al.. 2013 The 21-cm signature of the first stars during the Lyman-Werner feedback era. *MNRAS* **432**, 2909–2916. ([10.1093/mnras/stt650](https://doi.org/10.1093/mnras/stt650))
40. Fialkov A, Barkana R, Pinhas A et al.. 2014a Complete history of the observable 21 cm signal from the first stars during the pre-reionization era. *MNRAS* **437**, L36–L40. ([10.1093/mnrasl/slt135](https://doi.org/10.1093/mnrasl/slt135))
41. Fialkov A, Barkana R, Visbal E. 2014b The observable signature of late heating of the Universe during cosmic reionization. *Nature* **506**, 197–199. ([10.1038/nature12999](https://doi.org/10.1038/nature12999))
42. Fialkov A, Barkana R. 2014 The rich complexity of 21-cm fluctuations produced by the first stars. *MNRAS* **445**, 213–224. ([10.1093/mnras/stu1744](https://doi.org/10.1093/mnras/stu1744))
43. Fialkov A, Barkana R, Cohen A. 2015 Reconstructing the Nature of the First Cosmic Sources from the Anisotropic 21-cm Signal. *Phys. Rev. Lett.* **114**, 101303. ([10.1103/PhysRevLett.114.101303](https://doi.org/10.1103/PhysRevLett.114.101303))
44. Cohen A, Fialkov A, Barkana R. 2016 The 21-cm BAO signature of enriched low-mass galaxies during cosmic reionization. *MNRAS* **459**, L90–L94. ([10.1093/mnrasl/slw047](https://doi.org/10.1093/mnrasl/slw047))
45. Fialkov A, Cohen A, Barkana R et al.. 2017 Constraining the redshifted 21-cm signal with the unresolved soft X-ray background. *MNRAS* **464**, 3498–3508. ([10.1093/mnras/stw2540](https://doi.org/10.1093/mnras/stw2540))
46. Fialkov A, Barkana R, Cohen A. 2018 Constraining Baryon-Dark-Matter Scattering with the Cosmic Dawn 21-cm Signal. *Phys. Rev. Lett.* **121**, 011101. ([10.1103/PhysRevLett.121.011101](https://doi.org/10.1103/PhysRevLett.121.011101))
47. Fialkov A, Barkana R. 2019 Signature of excess radio background in the 21-cm global signal and power spectrum. *MNRAS* **486**, 1763–1773. ([10.1093/mnras/stz873](https://doi.org/10.1093/mnras/stz873))
48. Reis I, Fialkov A, Barkana R. 2020 High-redshift radio galaxies: a potential new source of 21-cm fluctuations. *MNRAS* **499**, 5993–6008. ([10.1093/mnras/staa3091](https://doi.org/10.1093/mnras/staa3091))
49. Reis I, Fialkov A, Barkana R. 2021 The subtlety of Ly α photons: changing the expected range of the 21-cm signal. *MNRAS* **506**, 5479–5493. ([10.1093/mnras/stab2089](https://doi.org/10.1093/mnras/stab2089))
50. Reis I, Barkana R, Fialkov A. 2022 Shot noise and scatter in the star formation efficiency as a source of 21-cm fluctuations. *MNRAS* **511**, 5265–5273. ([10.1093/mnras/stac411](https://doi.org/10.1093/mnras/stac411))
51. Magg M, Reis I, Fialkov A et al.. 2022 Effect of the cosmological transition to metal-enriched star formation on the hydrogen 21-cm signal. *MNRAS* **514**, 4433–4449. ([10.1093/mnras/stac1664](https://doi.org/10.1093/mnras/stac1664))
52. Gessey-Jones T, Sartorio NS, Fialkov A et al.. 2022 Impact of the primordial stellar initial mass function on the 21-cm signal. *MNRAS* **516**, 841–860. ([10.1093/mnras/stac2049](https://doi.org/10.1093/mnras/stac2049))
53. Sikder S, Barkana R, Fialkov A et al.. 2023 Strong 21-cm fluctuations and anisotropy due to the line-of-sight effect of radio galaxies at cosmic dawn. *MNRAS*. ([10.1093/mnras/stad3847](https://doi.org/10.1093/mnras/stad3847))

54. Gessey-Jones T, Fialkov A, de Lera Acedo E et al.. 2023 Signatures of cosmic ray heating in 21-cm observables. *MNRAS* **526**, 4262–4284. ([10.1093/mnras/stad3014](https://doi.org/10.1093/mnras/stad3014))
55. Acharya SK, Dhandha J, Chluba J. 2022 Can accreting primordial black holes explain the excess radio background?. *MNRAS* **517**, 2454–2461. ([10.1093/mnras/stac2739](https://doi.org/10.1093/mnras/stac2739))
56. Planck Collaboration, Aghanim N, Akrami Y et al.. 2020 Planck 2018 results. VI. Cosmological parameters. *A&A* **641**, A6. ([10.1051/0004-6361/201833910](https://doi.org/10.1051/0004-6361/201833910))
57. Park J, Mesinger A, Greig B et al.. 2019 Inferring the astrophysics of reionization and cosmic dawn from galaxy luminosity functions and the 21-cm signal. *MNRAS* **484**, 933–949. ([10.1093/mnras/stz032](https://doi.org/10.1093/mnras/stz032))
58. Furlanetto SR, Zaldarriaga M, Hernquist L. 2004 The Growth of H II Regions During Reionization. *ApJ* **613**, 1–15. ([10.1086/423025](https://doi.org/10.1086/423025))
59. Lewis A, Challinor A. 2007 21cm angular-power spectrum from the dark ages. *Phys. Rev. D* **76**, 083005. ([10.1103/PhysRevD.76.083005](https://doi.org/10.1103/PhysRevD.76.083005))
60. Ali-Haïmoud Y, Meerburg PD, Yuan S. 2014 New light on 21 cm intensity fluctuations from the dark ages. *Phys. Rev. D* **89**, 083506. ([10.1103/PhysRevD.89.083506](https://doi.org/10.1103/PhysRevD.89.083506))
61. Mondal R, Barkana R. 2023 Prospects for precision cosmology with the 21 cm signal from the dark ages. *Nature Astronomy* **7**, 1025–1030. ([10.1038/s41550-023-02057-y](https://doi.org/10.1038/s41550-023-02057-y))
62. Klessen RS, Glover SCO. 2023 The First Stars: Formation, Properties, and Impact. *ARA&A* **61**, 65–130. ([10.1146/annurev-astro-071221-053453](https://doi.org/10.1146/annurev-astro-071221-053453))
63. Wouthuysen SA. 1952 On the excitation mechanism of the 21-cm (radio-frequency) interstellar hydrogen emission line.. *AJ* **57**, 31–32. ([10.1086/106661](https://doi.org/10.1086/106661))
64. Field GB. 1958 Excitation of the Hydrogen 21-CM Line. *Proceedings of the IRE* **46**, 240–250. ([10.1109/JRPROC.1958.286741](https://doi.org/10.1109/JRPROC.1958.286741))
65. Fragos T, Lehmer BD, Naoz S et al.. 2013 Energy Feedback from X-Ray Binaries in the Early Universe. *ApJ* **776**, L31. ([10.1088/2041-8205/776/2/L31](https://doi.org/10.1088/2041-8205/776/2/L31))
66. Sartorio NS, Fialkov A, Hartwig T et al.. 2023 Population III X-ray binaries and their impact on the early universe. *MNRAS* **521**, 4039–4055. ([10.1093/mnras/stad697](https://doi.org/10.1093/mnras/stad697))
67. Madau P, Rees MJ. 2001 Massive Black Holes as Population III Remnants. *ApJ* **551**, L27–L30. ([10.1086/319848](https://doi.org/10.1086/319848))
68. Haiman Z, Loeb A. 2001 What Is the Highest Plausible Redshift of Luminous Quasars?. *ApJ* **552**, 459–463. ([10.1086/320586](https://doi.org/10.1086/320586))
69. Liu B, Sartorio NS, Izzard RG et al.. 2024 Population synthesis of Be X-ray binaries: metallicity dependence of total X-ray outputs. *MNRAS* **527**, 5023–5048. ([10.1093/mnras/stad3475](https://doi.org/10.1093/mnras/stad3475))
70. Pritchard JR, Furlanetto SR. 2007 21-cm fluctuations from inhomogeneous X-ray heating before reionization. *MNRAS* **376**, 1680–1694. ([10.1111/j.1365-2966.2007.11519.x](https://doi.org/10.1111/j.1365-2966.2007.11519.x))
71. Sazonov S, Sunyaev R. 2015 Preheating of the Universe by cosmic rays from primordial supernovae at the beginning of cosmic reionization. *MNRAS* **454**, 3464–3471. ([10.1093/mnras/stv2255](https://doi.org/10.1093/mnras/stv2255))
72. Chen X, Miralda-Escudé J. 2004 The Spin-Kinetic Temperature Coupling and the Heating Rate due to Ly α Scattering before Reionization: Predictions for 21 Centimeter Emission and Absorption. *ApJ* **602**, 1–11. ([10.1086/380829](https://doi.org/10.1086/380829))
73. Chuzhoy L, Shapiro PR. 2007 Heating and Cooling of the Early Intergalactic Medium by Resonance Photons. *ApJ* **655**, 843–846. ([10.1086/510146](https://doi.org/10.1086/510146))
74. Cohen A, Fialkov A, Barkana R et al.. 2017 Charting the parameter space of the global 21-cm signal. *MNRAS* **472**, 1915–1931. ([10.1093/mnras/stx2065](https://doi.org/10.1093/mnras/stx2065))
75. Barkana R, Loeb A. 2005 Probing the epoch of early baryonic infall through 21-cm fluctuations. *MNRAS* **363**, L36–L40. ([10.1111/j.1745-3933.2005.00079.x](https://doi.org/10.1111/j.1745-3933.2005.00079.x))
76. Bowman JD, Rogers AEE, Monsalve RA et al.. 2018 An absorption profile centred at 78 megahertz in the sky-averaged spectrum. *Nature* **555**, 67–70. ([10.1038/nature25792](https://doi.org/10.1038/nature25792))
77. Monsalve RA, Altamirano C, Bidula V et al.. 2023 Mapper of the IGM Spin Temperature (MIST): Instrument Overview. *arXiv e-prints* p. arXiv:2309.02996. ([10.48550/arXiv.2309.02996](https://doi.org/10.48550/arXiv.2309.02996))
78. de Lera Acedo E, de Villiers DIL, Razavi-Ghods N et al.. 2022 The REACH radiometer for detecting the 21-cm hydrogen signal from redshift $z \approx 7.5$ –28. *Nature Astronomy* **6**, 984–998. ([10.1038/s41550-022-01709-9](https://doi.org/10.1038/s41550-022-01709-9))
79. Singh S, Jishnu NT, Subrahmanyan R et al.. 2022 On the detection of a cosmic dawn signal in the radio background. *Nature Astronomy* **6**, 607–617. ([10.1038/s41550-022-01610-5](https://doi.org/10.1038/s41550-022-01610-5))
80. Abdurashidova Z, Aguirre JE, Alexander P et al.. 2022 First Results from HERA Phase I: Upper Limits on the Epoch of Reionization 21 cm Power Spectrum. *ApJ* **925**, 221. ([10.3847/1538-4357/ac1c78](https://doi.org/10.3847/1538-4357/ac1c78))

81. Gehlot BK, Mertens FG, Koopmans LVE et al.. 2019 The first power spectrum limit on the 21-cm signal of neutral hydrogen during the Cosmic Dawn at $z = 20$ –25 from LOFAR. *MNRAS* **488**, 4271–4287. ([10.1093/mnras/stz1937](https://doi.org/10.1093/mnras/stz1937))
82. Mertens FG, Mevius M, Koopmans LVE et al.. 2020 Improved upper limits on the 21 cm signal power spectrum of neutral hydrogen at $z \approx 9.1$ from LOFAR. *MNRAS* **493**, 1662–1685. ([10.1093/mnras/staa327](https://doi.org/10.1093/mnras/staa327))
83. Mertens FG, Semelin B, Koopmans LVE. 2021 Exploring the Cosmic Dawn with NenuFAR. In Siebert A, Baillié K, Lagadec E, Lagarde N, Malzac J, Marquette JB, N'Diaye M, Richard J, Venot O, editors, *SF2A-2021: Proceedings of the Annual meeting of the French Society of Astronomy and Astrophysics* pp. 211–214. ([10.48550/arXiv.2109.10055](https://doi.org/10.48550/arXiv.2109.10055))
84. Munshi S, Mertens FG, Koopmans LVE et al.. 2023 First upper limits on the 21-cm signal power spectrum from the Cosmic Dawn from one night of observations with NenuFAR. *arXiv e-prints* p. arXiv:2311.05364. ([10.48550/arXiv.2311.05364](https://doi.org/10.48550/arXiv.2311.05364))
85. Ewall-Wice A, Dillon JS, Hewitt JN et al.. 2016 First limits on the 21 cm power spectrum during the Epoch of X-ray heating. *MNRAS* **460**, 4320–4347. ([10.1093/mnras/stw1022](https://doi.org/10.1093/mnras/stw1022))
86. Eastwood MW, Anderson MM, Monroe RM et al.. 2019 The 21 cm Power Spectrum from the Cosmic Dawn: First Results from the OVRO-LWA. *AJ* **158**, 84. ([10.3847/1538-3881/ab2629](https://doi.org/10.3847/1538-3881/ab2629))
87. Garsden H, Greenhill L, Bernardi G et al.. 2021 A 21-cm power spectrum at 48 MHz, using the Owens Valley Long Wavelength Array. *MNRAS* **506**, 5802–5817. ([10.1093/mnras/stab1671](https://doi.org/10.1093/mnras/stab1671))
88. Dewdney PE, Hall PJ, Schilizzi RT et al.. 2009 The Square Kilometre Array. *IEEE Proceedings* **97**, 1482–1496. ([10.1109/JPROC.2009.2021005](https://doi.org/10.1109/JPROC.2009.2021005))
89. Koopmans L, Pritchard J, Mellema G et al.. 2015 The Cosmic Dawn and Epoch of Reionisation with SKA. In *Advancing Astrophysics with the Square Kilometre Array (AASKA14)* p. 1. ([10.22323/1.215.0001](https://doi.org/10.22323/1.215.0001))
90. Barkana R. 2018 Possible interaction between baryons and dark-matter particles revealed by the first stars. *Nature* **555**, 71–74. ([10.1038/nature25791](https://doi.org/10.1038/nature25791))
91. Muñoz JB, Loeb A. 2018 A small amount of mini-charged dark matter could cool the baryons in the early Universe. *Nature* **557**, 684–686. ([10.1038/s41586-018-0151-x](https://doi.org/10.1038/s41586-018-0151-x))
92. Kovetz ED, Poulin V, Gluscevic V et al.. 2018 Tighter limits on dark matter explanations of the anomalous EDGES 21 cm signal. *Phys. Rev. D* **98**, 103529. ([10.1103/PhysRevD.98.103529](https://doi.org/10.1103/PhysRevD.98.103529))
93. Liu H, Outmezguine NJ, Redigolo D et al.. 2019 Reviving millicharged dark matter for 21-cm cosmology. *Phys. Rev. D* **100**, 123011. ([10.1103/PhysRevD.100.123011](https://doi.org/10.1103/PhysRevD.100.123011))
94. Feng C, Holder G. 2018 Enhanced Global Signal of Neutral Hydrogen Due to Excess Radiation at Cosmic Dawn. *ApJ* **858**, L17. ([10.3847/2041-8213/aac0fe](https://doi.org/10.3847/2041-8213/aac0fe))
95. Ewall-Wice A, Chang TC, Lazio J et al.. 2018 Modeling the Radio Background from the First Black Holes at Cosmic Dawn: Implications for the 21 cm Absorption Amplitude. *ApJ* **868**, 63. ([10.3847/1538-4357/aae51d](https://doi.org/10.3847/1538-4357/aae51d))
96. Ewall-Wice A, Chang TC, Lazio TJW. 2020 The Radio Scream from black holes at Cosmic Dawn: a semi-analytic model for the impact of radio-loud black holes on the 21 cm global signal. *MNRAS* **492**, 6086–6104. ([10.1093/mnras/stz3501](https://doi.org/10.1093/mnras/stz3501))
97. Bale SD, Bassett N, Burns JO et al.. 2023 LuSEE 'Night': The Lunar Surface Electromagnetics Experiment. *arXiv e-prints* p. arXiv:2301.10345. ([10.48550/arXiv.2301.10345](https://doi.org/10.48550/arXiv.2301.10345))
98. Bilitza D, Pezzopane M, Truhlik V et al.. 2022 The International Reference Ionosphere Model: A Review and Description of an Ionospheric Benchmark. *Reviews of Geophysics* **60**, e2022RG000792. ([10.1029/2022RG000792](https://doi.org/10.1029/2022RG000792))
99. Vedantham HK, Koopmans LVE, de Bruyn AG et al.. 2014 Chromatic effects in the 21 cm global signal from the cosmic dawn. *MNRAS* **437**, 1056–1069. ([10.1093/mnras/stt1878](https://doi.org/10.1093/mnras/stt1878))
100. Shen E, Anstey D, de Lera Acedo E et al.. 2021 Quantifying ionospheric effects on global 21-cm observations. *MNRAS* **503**, 344–353. ([10.1093/mnras/stab429](https://doi.org/10.1093/mnras/stab429))
101. Shen E, Anstey D, de Lera Acedo E et al.. 2022 Bayesian data analysis for sky-averaged 21-cm experiments in the presence of ionospheric effects. *MNRAS* **515**, 4565–4573. ([10.1093/mnras/stac1900](https://doi.org/10.1093/mnras/stac1900))
102. Mevius M, van der Tol S, Pandey VN et al.. 2016 Probing ionospheric structures using the LOFAR radio telescope. *Radio Science* **51**, 927–941. ([10.1002/2016RS006028](https://doi.org/10.1002/2016RS006028))
103. Edler HW, de Gasperin F, Rafferty D. 2021 Investigating ionospheric calibration for LOFAR 2.0 with simulated observations. *A&A* **652**, A37. ([10.1051/0004-6361/202140465](https://doi.org/10.1051/0004-6361/202140465))
104. Anstey D, de Lera Acedo E, Handley W. 2021 A general Bayesian framework for foreground modelling and chromaticity correction for global 21 cm experiments. *MNRAS* **506**, 2041–2058. ([10.1093/mnras/stab1765](https://doi.org/10.1093/mnras/stab1765))

105. Bevins HTJ, Heimersheim S, Abril-Cabezas I et al.. 2023 Joint analysis constraints on the physics of the first galaxies with low frequency radio astronomy data. *MNRAS*. ([10.1093/mnras/stad3194](https://doi.org/10.1093/mnras/stad3194))
106. HERA Collaboration, Abdurashidova Z, Adams T et al.. 2023 Improved Constraints on the 21 cm EoR Power Spectrum and the X-Ray Heating of the IGM with HERA Phase I Observations. *ApJ* **945**, 124. ([10.3847/1538-4357/acaf50](https://doi.org/10.3847/1538-4357/acaf50))
107. Ghara R, Giri SK, Mellema G et al.. 2020 Constraining the intergalactic medium at $z \approx 9.1$ using LOFAR Epoch of Reionization observations. *MNRAS* **493**, 4728–4747. ([10.1093/mnras/staa487](https://doi.org/10.1093/mnras/staa487))
108. Trott CM, Jordan CH, Midgley S et al.. 2020 Deep multiredshift limits on Epoch of Reionization 21 cm power spectra from four seasons of Murchison Widefield Array observations. *MNRAS* **493**, 4711–4727. ([10.1093/mnras/staa414](https://doi.org/10.1093/mnras/staa414))
109. Bevins HTJ, de Lera Acedo E, Fialkov A et al.. 2022 A comprehensive Bayesian reanalysis of the SARAS2 data from the epoch of reionization. *MNRAS* **513**, 4507–4526. ([10.1093/mnras/stac1158](https://doi.org/10.1093/mnras/stac1158))
110. Monsalve RA, Rogers AEE, Bowman JD et al.. 2017 Results from EDGES High-band. I. Constraints on Phenomenological Models for the Global 21 cm Signal. *ApJ* **847**, 64. ([10.3847/1538-4357/aa88d1](https://doi.org/10.3847/1538-4357/aa88d1))
111. Monsalve RA, Greig B, Bowman JD et al.. 2018 Results from EDGES High-band. II. Constraints on Parameters of Early Galaxies. *ApJ* **863**, 11. ([10.3847/1538-4357/aace54](https://doi.org/10.3847/1538-4357/aace54))
112. Monsalve RA, Fialkov A, Bowman JD et al.. 2019 Results from EDGES High-Band. III. New Constraints on Parameters of the Early Universe. *ApJ* **875**, 67. ([10.3847/1538-4357/ab07be](https://doi.org/10.3847/1538-4357/ab07be))
113. Gehlot BK, Mertens FG, Koopmans LVE et al.. 2020 The AARTFAAC Cosmic Explorer: observations of the 21-cm power spectrum in the EDGES absorption trough. *MNRAS* **499**, 4158–4173. ([10.1093/mnras/staa3093](https://doi.org/10.1093/mnras/staa3093))
114. Yoshiura S, Pindor B, Line JLB et al.. 2021 A new MWA limit on the 21 cm power spectrum at redshifts 13–17. *MNRAS* **505**, 4775–4790. ([10.1093/mnras/stab1560](https://doi.org/10.1093/mnras/stab1560))
115. Hickox RC, Markevitch M. 2006 Absolute Measurement of the Unresolved Cosmic X-Ray Background in the 0.5–8 keV Band with Chandra. *ApJ* **645**, 95–114. ([10.1086/504070](https://doi.org/10.1086/504070))
116. Harrison FA, Aird J, Civano F et al.. 2016 The NuSTAR Extragalactic Surveys: The Number Counts of Active Galactic Nuclei and the Resolved Fraction of the Cosmic X-Ray Background. *ApJ* **831**, 185. ([10.3847/0004-637X/831/2/185](https://doi.org/10.3847/0004-637X/831/2/185))
117. Fixsen DJ, Kogut A, Levin S et al.. 2011 ARCADE 2 Measurement of the Absolute Sky Brightness at 3–90 GHz. *ApJ* **734**, 5. ([10.1088/0004-637X/734/1/5](https://doi.org/10.1088/0004-637X/734/1/5))
118. Dowell J, Taylor GB. 2018 The Radio Background below 100 MHz. *ApJ* **858**, L9. ([10.3847/2041-8213/aabf86](https://doi.org/10.3847/2041-8213/aabf86))
119. Pochinda S, Gessey-Jones T, Bevins HTJ et al.. 2023 Constraining the properties of Population III galaxies with multi-wavelength observations. *arXiv e-prints* p. arXiv:2312.08095. ([10.48550/arXiv.2312.08095](https://doi.org/10.48550/arXiv.2312.08095))
120. Schaerer D. 2002 On the properties of massive Population III stars and metal-free stellar populations. *A&A* **382**, 28–42. ([10.1051/0004-6361:20011619](https://doi.org/10.1051/0004-6361:20011619))
121. Cole PS, Silk J. 2021 Small-scale primordial fluctuations in the 21 cm Dark Ages signal. *MNRAS* **501**, 2627–2634. ([10.1093/mnras/staa3638](https://doi.org/10.1093/mnras/staa3638))
122. Cumberbatch DT, Lattanzi M, Silk J. 2010 Signatures of clumpy dark matter in the global 21 cm background signal. *Phys. Rev. D* **82**, 103508. ([10.1103/PhysRevD.82.103508](https://doi.org/10.1103/PhysRevD.82.103508))
123. Pillepich A, Porciani C, Matarrese S. 2007 The Bispectrum of Redshifted 21 Centimeter Fluctuations from the Dark Ages. *ApJ* **662**, 1–14. ([10.1086/517963](https://doi.org/10.1086/517963))
124. Cooray A. 2006 21-cm Background Anisotropies Can Discern Primordial Non-Gaussianity. *Phys. Rev. Lett.* **97**, 261301. ([10.1103/PhysRevLett.97.261301](https://doi.org/10.1103/PhysRevLett.97.261301))
125. Flöss T, de Wild T, Meerburg PD et al.. 2022 The Dark Ages' 21-cm trispectrum. *J. Cosmology Astropart. Phys.* **2022**, 020. ([10.1088/1475-7516/2022/06/020](https://doi.org/10.1088/1475-7516/2022/06/020))
126. Orlando G, Flöss T, Meerburg PD et al.. 2023 Local non-Gaussianities from cross-correlations between the CMB and 21-cm. *arXiv e-prints* p. arXiv:2307.15046. ([10.48550/arXiv.2307.15046](https://doi.org/10.48550/arXiv.2307.15046))
127. Muñoz JB, Ali-Haïmoud Y, Kamionkowski M. 2015 Primordial non-gaussianity from the bispectrum of 21-cm fluctuations in the dark ages. *Phys. Rev. D* **92**, 083508. ([10.1103/PhysRevD.92.083508](https://doi.org/10.1103/PhysRevD.92.083508))
128. Tashiro H, Kadota K, Silk J. 2014 Effects of dark matter-baryon scattering on redshifted 21 cm signals. *Phys. Rev. D* **90**, 083522. ([10.1103/PhysRevD.90.083522](https://doi.org/10.1103/PhysRevD.90.083522))

129. Hiroshima N, Kohri K, Sekiguchi T et al.. 2021 Impacts of new small-scale N - body simulations on dark matter annihilations constrained from cosmological 21-cm line observations. *Phys. Rev. D* **104**, 083547. ([10.1103/PhysRevD.104.083547](https://doi.org/10.1103/PhysRevD.104.083547))
130. Slatyer TR, Wu CL. 2018 Early-Universe constraints on dark matter-baryon scattering and their implications for a global 21 cm signal. *Phys. Rev. D* **98**, 023013. ([10.1103/PhysRevD.98.023013](https://doi.org/10.1103/PhysRevD.98.023013))
131. Short K, Bernal JL, Raccanelli A et al.. 2020 Enlightening the dark ages with dark matter. *J. Cosmology Astropart. Phys.* **2020**, 020. ([10.1088/1475-7516/2020/07/020](https://doi.org/10.1088/1475-7516/2020/07/020))
132. Mondal R, Barkana R, Fialkov A. 2023 Constraining exotic dark matter models with the dark ages 21-cm signal. *arXiv e-prints* p. arXiv:2310.15530. ([10.48550/arXiv.2310.15530](https://arxiv.org/abs/2310.15530))
133. Vanzan E, Raccanelli A, Bartolo N. 2023 Dark ages, a window on the dark sector. Hunting for ultra-light axions. *arXiv e-prints* p. arXiv:2306.09252. ([10.48550/arXiv.2306.09252](https://arxiv.org/abs/2306.09252))
134. Mack KJ, Wesley DH. 2008 Primordial black holes in the Dark Ages: Observational prospects for future 21cm surveys. *arXiv e-prints* p. arXiv:0805.1531. ([10.48550/arXiv.0805.1531](https://arxiv.org/abs/0805.1531))
135. Thériault R, Mirocha JT, Brandenberger R. 2021 Global 21cm absorption signal from superconducting cosmic strings. *J. Cosmology Astropart. Phys.* **2021**, 046. ([10.1088/1475-7516/2021/10/046](https://doi.org/10.1088/1475-7516/2021/10/046))
136. Yang Y. 2022 Impact of radiation from primordial black holes on the 21-cm angular-power spectrum in the dark ages. *Phys. Rev. D* **106**, 123508. ([10.1103/PhysRevD.106.123508](https://doi.org/10.1103/PhysRevD.106.123508))
137. Kobayashi T, Takahashi F. 2011 Running spectral index from inflation with modulations. *J. Cosmology Astropart. Phys.* **2011**, 026. ([10.1088/1475-7516/2011/01/026](https://doi.org/10.1088/1475-7516/2011/01/026))
138. Acharya SK, Dhandha J, Chluba J. 2022 Can accreting primordial black holes explain the excess radio background?. *MNRAS* **517**, 2454–2461. ([10.1093/mnras/stac2739](https://doi.org/10.1093/mnras/stac2739))
139. Burns J, Bale S, Bradley R et al.. 2021 Global 21-cm Cosmology from the Farside of the Moon. *arXiv e-prints* p. arXiv:2103.05085. ([10.48550/arXiv.2103.05085](https://arxiv.org/abs/2103.05085))
140. Koopmans LVE, Barkana R, Bentum M et al.. 2021 Peering into the dark (ages) with low-frequency space interferometers. *Experimental Astronomy* **51**, 1641–1676. ([10.1007/s10686-021-09743-7](https://doi.org/10.1007/s10686-021-09743-7))
141. Grimm RE. 2018 New analysis of the Apollo 17 surface electrical properties experiment. *Icarus* **314**, 389–399. ([10.1016/j.icarus.2018.06.007](https://doi.org/10.1016/j.icarus.2018.06.007))
142. Gamsky JN, Metzger PT. 2023 The Physical State of Lunar Soil in the Permanently Shadowed Craters of the Moon. *arXiv e-prints* p. arXiv:2305.20007. ([10.48550/arXiv.2305.20007](https://arxiv.org/abs/2305.20007))
143. Grün E, Horanyi M, Sternovsky Z. 2011 The lunar dust environment. *Planet. Space Sci.* **59**, 1672–1680. ([10.1016/j.pss.2011.04.005](https://doi.org/10.1016/j.pss.2011.04.005))
144. Klein Wolt M, Aminaei A, Pourshaghghi H et al.. 2013 Low-frequency cosmology from the moon. In *European Planetary Science Congress* pp. EPSC2013–152.
145. Le Conte ZA, Elvis M, Gläser PA. 2023 Lunar far-side radio arrays: a preliminary site survey. *RAS Techniques and Instruments* **2**, 360–377. ([10.1093/rasti/rzad022](https://doi.org/10.1093/rasti/rzad022))